$$I = K_1 \int_{z_f}^{z_i} \frac{V'}{(\rho)^{1/2} V} dz \tag{19}$$

with the condition $x = l$. For the lifting entry with minimum heat yielded in the critical zone (denoting by K_2 another constant) one must find the minimum of the functional

$$I^* = K_2 \int_{z_f}^{z_i} \frac{VV'}{(\rho)^{1/2}} dz \tag{20}$$

with the same condition. Both problems may be solved in this manner.

References

[1] Marinescu, A., "Sur l'optimisation de l'entrée des engins spatiaux dans l'atmosphère planetaire," *Rendiconti Accademia Nazionale dei Lincei*, Vol. LI, Fasc. 5, Nov. 1971.

Laminar Boundary Layer in Noncentered Unsteady Waves

J. GORDON HALL,* G. SRINIVASAN,† AND JAIPAL S. RATHI†
State University of New York at Buffalo, Buffalo, N.Y.

PREVIOUS analyses[1,2] have considered the laminar wall boundary layer developed within unsteady simple waves which are centered. The present Note concerns the influence of noncentered wave forms which typically occur in practice. A more detailed account is given in Ref. 3.

Figure 1 shows the straight-line mathematical characteristics in the distance-time or x, t plane for inviscid flow generated by simple expansion or compression waves.[4] The wavehead moves at constant sound speed a_0 towards $-x$ into uniform, stationary, perfect gas of constant specific heat ratio γ. The relation $(\gamma-1)u_e/2 + a_e = a_0$ applies locally, and flow properties are constant along the straight characteristics which have slopes $dx/dt = u_e - a_e = u_e/\beta - a_0$ where u = velocity along x, a = sound speed, $\beta = 2/(\gamma+1)$, and subscripts e and 0 denote inviscid flow and gas ahead of the wave, respectively. The first derivatives of the flow properties are assumed to be initially discontinuous, i.e., to be nonzero immediately after the wavehead (cf. Fig. 2). This requires that the wave be generated with nonzero initial acceleration of the gas (say by suitable piston motion or diaphragm rupture). It then follows[3] that the wavehead first derivatives (subscript H) satisfy $(\partial p/\partial t)_H = a_0(\partial p/\partial x)_H = -\gamma\beta p_0/t$ and $(\partial u_e/\partial t)_H = a_0(\partial u_e/\partial x)_H = -\beta a_0/t$. Thus the wavehead first derivatives at any x [say $(\partial p/\partial t)_H$ as measured from Fig. 2] automatically define the corresponding time t and thus uniquely locate the origin of x, t along the wavehead path. The preceding wavehead relations for noncentered waves apply throughout the entire flow within centered waves.

In Fig. 1, e is the x-axis intercept of the straight characteristic through x, t and also represents the x displacement of the local particle at x, t from its position in a centered wave for given velocity u_e. To any point x, t there corresponds a unique value of e determined only by u_e, i.e., $(x-e)/t = u_e/\beta - a_0$. The noncentered flow is thus completely defined by specifying $e(u_e)$. It can be shown[3] that de/du_e as well as e must vanish at the wavehead. In general, e may be $\gtrless 0$. Thus a constant acceleration piston gives $e > 0$ for compression waves and $e < 0$ for expansion waves. In experiments with simple waves $e(u_e)$ can be determined from a record of $u_e(t)$ or $p_e(t)$ obtained at any x location.[3] For example, the measured pressure-time history of Fig. 2 for a diaphragm-generated expansion wave gives the determination of $e(u_e)$ shown in Fig. 3.

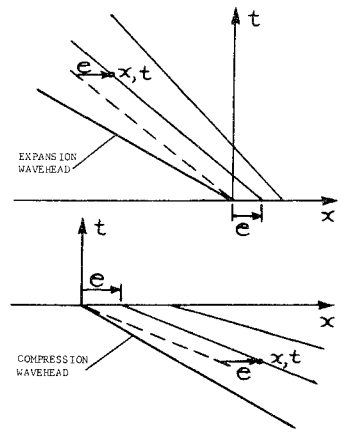

Fig. 1 Distance-time or x, t diagram of straight characteristics for simple noncentered waves.

If e is regarded as a function of x and t a new independent variable $s(x, t)$ can be defined as $s = 1 + x/a_0t - e/a_0t = s^* - e/a_0t$. s provides a local conical similarity for the inviscid flow in noncentered waves analogous to s^* for centered waves (where $e \equiv 0$). With centered waves s^* is the ratio of the x distance of any point x, t from the wavehead to the distance of the wavehead from the wave focal point. In terms of s the inviscid flow variables are given by $u_e = \beta a_0 s$ and $(p_e/p_0)^{e/\gamma\beta} = (\rho_e/\rho_0)^{e/\beta} = (T_e/T_0)^{1/2} = a_e/a_0 = 1 - \varepsilon s$, where ρ is density, T is absolute temperature, and $\varepsilon = (\gamma-1)/(\gamma+1)$. s is > 0 for expansion waves and < 0 for compression waves; its magnitude increases monotonically from zero at the wavehead where $x = -a_0t$ and $e = 0$. Although the magnitude of e/a_0t will typically be small, e itself is unrestricted.

Transformation and Solution of Boundary-Layer Equations

The T, ρ, p, and u-velocity fields outside the gas boundary layer are assumed to be those of the noncentered wave discussed. The initial gas boundary layer ($y \geqq 0$, y = distance normal to wall) is described by the customary approximations for two-dimensional, unsteady, compressible laminar boundary layers with heat transfer. Gas viscosity μ is assumed proportional to T; local $\rho\mu$ is thus proportional to $p = p_e(x, t)$. Heat transfer also produces a thin thermal boundary layer in the homo-

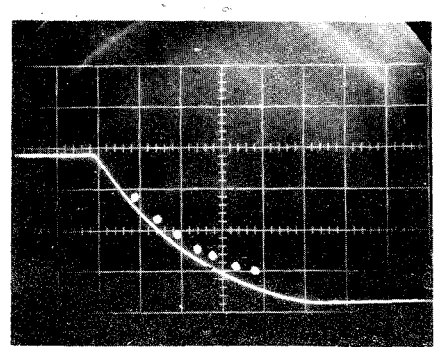

Fig. 2 Oscilloscope trace of sidewall static pressure vs time for expansion wave. 10 psi/cm vertical and 0.5 msec/cm horizontal. Dots indicate centered-wave values. Air with $p_0 = 85$ psi, $T_0 = 74°$F. Kistler 603A transducer 3 ft from diaphragm. Tube is $1\frac{1}{2}$ in. × 5 in. cross section. Flow discharges to room through choked 1 in. × 5 in. slot orifice plate at tube end.

Received May 14, 1973. This work was supported by ONR under Contract N00014-72-C0373.

Index categories: Boundary Layers and Convective Heat Transfer—Laminar; Nonsteady Aerodynamics.

* Professor, Department of Mechanical Engineering.

† Research Assistant.

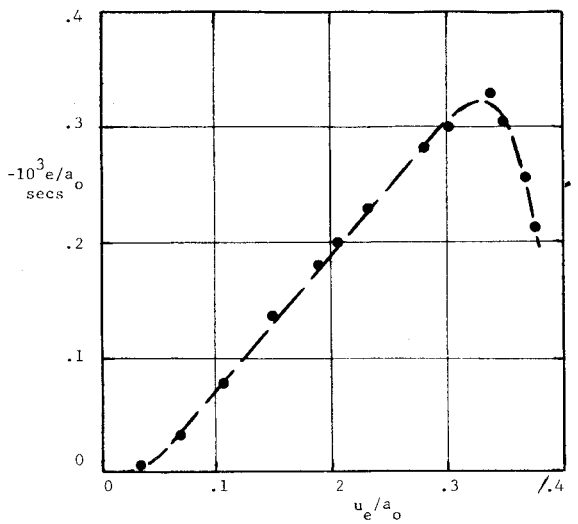

Fig. 3 Function $e(u_e)$ determined from pressure record of Fig. 2.

geneous wall ($y \leqq 0$). Temperature θ in the wall is governed by the approximate heat-conduction equation $\partial\theta/\partial t = \alpha\partial^2\theta/\partial y^2$, where α = wall thermal diffusivity. The assumed y boundary conditions are: at $y = \infty$, $u = u_e$ and $T = T_e$; at $y = 0$, $u = v$ (= gas velocity along y) $= 0$ and $T = \theta = T_w(x,t)$; and at $y = -\infty$, $\theta = T_0$. The wall surface temperature $T_w(x,t)$ is unknown, and its determination in the over-all solution requires matching local gas and wall heat-transfer rates at $y = 0$, i.e., $q_w = -k_w(\partial T/\partial y)_{y=0} = -k_B(\partial\theta/\partial y)_{y=0}$ where k is thermal conductivity and subscripts B and W denote wall material and gas conditions at $y = 0$, respectively. At the wavehead the gas is at rest and $\theta = T = T_0$.

The governing equations are transformed in terms of new independent and dependent variables; the continuity equation is used to eliminate v from the x-momentum and gas energy equations. The new independent variables are s, $t' = t$, and a normal coordinate η defined by $\eta = [a_0/\nu_0(x+a_0t-e)]^{1/2} \int_0 (\rho/\rho_0)\, dy$ for $y > 0$ and $\eta = -y[a_0/\alpha(x+a_0t-e)]^{1/2}$ for $y < 0$, where $\nu = \mu/\rho$. The new dependent variables are F, G, and H, defined by $u = u_e\partial F/\partial\eta$, $T = T_w+(T_e-T_w)G$, and $\theta = T_w+(T_0-T_w)H$. The transformed equations[3] constitute three nonlinear partial differential equations involving F, G, H, and $T_w(s,t')$, and an algebraic relation involving T_w and surface values of $\partial G/\partial\eta$ and $\partial H/\partial\eta$. The t' dependence appears only in a local inverse-time parameter $\omega = (\beta/t')\, de/du_e$ which depends implicitly on s as well as on t'.

ω must vanish at the wavehead and can be considered small compared to unity in the initial flow region.[3] The dependent functions can then be expressed as asymptotic series expansions in ascending powers of ω with coefficients $Y_i(s,\eta)$. For the initial flow region s is also small, and the Y_i can in turn be expressed as power series expansions in s. Thus $\partial F/\partial\eta$, G, and H are represented by $Y = \Sigma\omega^i Y_i = \Sigma\Sigma\omega^i Y_{ij} s^j$ where $Y_{ij} = Y_{ij}(\eta)$ and i,j take values 0, 1, 2, ... Similarly for the surface temperature, $T_w/T_0 = \Sigma\omega^i B_i = \Sigma\Sigma\omega^i B_{ij} s^j$ where $B_i = B_i(s)$ and B_{ij} = constant. Substitution into the transformed equations then leads to a sequence of linear ordinary differential equations for Y_{ij} (and algebraic equations for B_{ij}) of the form[3] $Y_{ij}'' + (z/2)Y_{ij}' - (i+j+1)Y_{ij} = \bar{Y}_{ij}$ where $Y_{ij}' = dY_{ij}/dz$, and Y_{ij} represents F_{ij}', G_{ij}, or H_{ij} with $z = \eta$, $\sigma^{1/2}\eta$, or η, respectively. The boundary conditions are $Y_{ij}(0) = Y_{ij}(\infty) = 0$ except for $Y_{00}(\infty) = 1$.

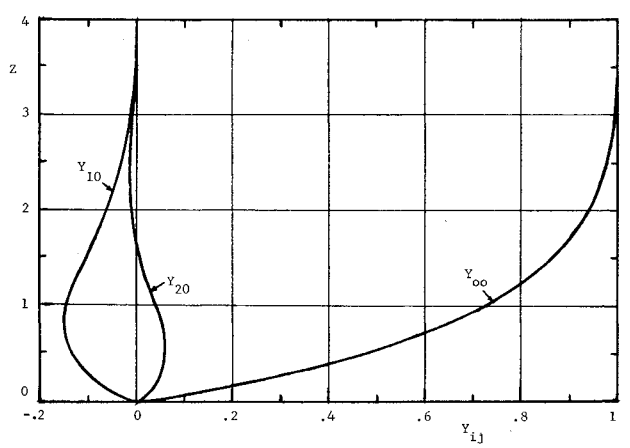

Fig. 4 Functions Y_{00}, Y_{10}, Y_{20}.

Results and Discussion

The function $\bar{Y}_{ij}$ denotes nonhomogeneous terms generally dependent on lower order functions and implicitly on $Y_{ij}'(0)$. The general solutions to the homogeneous equations are expressible in terms of repeated error function integrals. However, for $j \geqq 1$ the $\bar{Y}_{ij}$ are sufficiently complicated that numerical methods are appropriate. The present consideration was limited to the zero-order solution ($i = 0$) and to the leading terms in ω and ω^2 ($i = 1$ and $2, j = 0$).

The zero-order equations are identical to those of Ref. 2 for the centered-wave problem with finite k_B or variable T_w. Consequently, the zero-order solution is given by the centered wave solution with the centered wave variables s^* and η^* replaced by s and η. Although the zero-order solution partially accounts for noncentered wave effects through s and η, a more complete solution requires higher-order terms in ω. The leading terms in ω and ω^2 are obtainable in closed form as follows[3]: $Y_{10} = (z^2/2)(1 + z^2/12)$ erf $c(z/2) - (5z/6\pi^{1/2})(1 + z^2/10)$ exp $(-z^2/4)$, and $Y_{20} = -(z^2/2)(1 + z^2/4 + z^4/120)$ erf $c(z/2) + (z/30\pi^{1/2})(129/8 + 7z^2 + z^4/4)\exp(-z^2/4)$ where Y_{i0} represents F_{i0}', G_{i0}, or H_{i0} with $z = \eta$, $\sigma^{1/2}\eta$, or η, respectively. The solutions for Y_{10} and Y_{20} are plotted in Fig. 4 along with the leading term of the zero-order solution $Y_{00} = 1-(1+z^2/2)$ erf $c(z/2) + z\pi^{-1/2}\exp(-z^2/4)$. As expected, the functions and their initial slopes become smaller as i increases. The initial slopes, which determine surface heat transfer and shear stress, have the values $Y_{00}'(0) = 2/\pi^{1/2}$, $Y_{10}'(0) = -5/6\pi^{1/2}$, $Y_{20}'(0) = 129/240\pi^{1/2}$.

For the B_{ij}, $B_{i0} = 0$ except for $B_{00} = 1$, and $B_{i1} = 0$ for $i \geqq 1$. The result for T_w is $T_w/T_0 = 1 + B_{01}s + B_{02}s^2 + \cdots + 0(\omega s^2)$. Thus the noncentered wave influence on T_w is largely accounted for by the zero-order solution $B_0(s)$. The first term in ω is of third order (ωs^2) in the quantities considered small. Considering only first-order terms, the fractional change in $T_w - T_0$ at given x and t caused by the noncentered wave form is $(T_w - T_w^*)/(T_w^* - T_0) \simeq (s - s^*)/s^* = -e/a_0 s^* t = -(1 + u_e t/\beta e)^{-1}$, where $T_w^*(x,t)$ is the centered-wave solution. For the expansion-wave example of Fig. 3, where $e < 0$ and $s > 0$, T_w is thus reduced below T_w^*. The maximum effect at distances of 3–4 ft from the origin, or t in the range of approximately 4 to 6 msec, is about 20–25%. The magnitude of the effect will vary approximately as $1/x$ or $1/t$.

The noncentered wave influence on the surface heat-transfer rate q_w is most readily evaluated for $k_B = \infty$ (T_w = const) for which $B_{0j} = 0$ and $G_{01}'(0) = 0.1507$ (Ref. 1) for $\sigma = 0.72$, $\gamma = 1.4$. Considering only leading terms, the fractional change in $q_w(x,t)$ is given approximately by[3] $(q_w - q_w^*)/q_w^* \simeq [\varepsilon/2 + \gamma\beta(1 - a_0/2\gamma u_e) - G_{01}'(0)/G_{00}'(0)]e/a_0 t + \omega G_{10}'(0)/G_{00}'(0)$ in the limit $k_B = \infty$, where $q_w^*(x,t)$ is the centered wave value. For the expansion wave of Fig. 3 both e and ω are negative at small s. Both right hand terms of $q_w - q_w^*$ are then positive, so that q_w is increased over q_w^* in that case. For t in the range of 4–6 msec the maximum increase in q_w is about 10–15% (varying approximately as $1/x$ or $1/t$). The results for skin friction are qualitatively similar to those for heat transfer but the noncentered wave effects are somewhat larger.[3]

In earlier shock-tube experiments[5] substantial discrepancies

were observed between measured values of T_w and q_w and the laminar boundary-layer theory for centered expansion waves. If the (unmeasured) waveforms were qualitatively similar to that of Fig. 2 then the observed discrepancies are at least qualitatively explained by the predictions of the present analysis.

References

[1] Cohen, N. B., "A Power Series Solution for the Unsteady Laminar Boundary Layer Flow in an Expansion Wave of Finite Width Moving Through a Gas Initially at Rest," TN3943, 1957, NACA.

[2] Hall, J. G., "Laminar Boundary Layers Developed within Unsteady Expansion and Compressions Waves," *AIAA Journal*, Vol. 10, No. 4, April 1972, pp. 499–505.

[3] Hall, J. G., Srinivasan, G., and Rathi, J. S., "Analysis of Laminar Boundary Layers in Non-Centered Unsteady Waves," FTSL TR 73-1, Feb. 1973, Fluid and Thermal Sciences Lab., State Univ. of New York at Buffalo, Buffalo, N.Y.

[4] Courant, R. and Friedrichs, K. O., *Supersonic Flow and Shock Waves*, Interscience, New York, 1948, Chap. III B.

[5] Chabai, A. J., "Measurement of Wall Heat Transfer and of Transition to Turbulence During Hot Gas and Rarefaction Flows in a Shock Tube," TR 12, Ph.D. thesis, 1958, Dept. of Physics, Lehigh Univ., Bethlehem, Pa.

Hot-Wire Coil Probe for High-Speed Flows

LEONARD M. WEINSTEIN*

NASA Langley Research Center, Hampton, Va.

Nomenclature

d	= diameter of wire
D	= diameter of coil
e	= compensated hot-wire output voltage
f	= frequency
h	= wire film coefficient of heat transfer
I	= hot-wire heating current
k	= thermal conductivity of gas
l	= length of wire
M	= Mach number
Nu_t	= hd/k_t = Nusselt number
$Re_{t,d}$ $Re_{t,D}$	= $(\rho U)_t d/\mu_t$ and $(\rho U)_t D/\mu_t$, respectively, Reynolds number
T	= temperature
U	= gas velocity
η	= wire recovery factor $(T_w/T_t$ as $I_w \to 0)$
μ	= gas viscosity
ρ	= gas density

Subscripts

∞	= freestream value
d	= based on wire diameter
D	= based on coil diameter
l	= local flow value
w	= hot wire
t	= local total value

Introduction

CONVENTIONAL hot-wire probes for high-speed flows typically have the wire mounted slack between end supports. This slack minimizes wire breakage, and reduces strain gage effects.[1] The wire length to diameter ratio and necessary amount of slack depend on the test environment, and are a compromise between end loss effects and strength. For high wire loading the wire may need to be so short that end conduction losses are large. In addition, the large amount of slack needed can result in wire support interference even when the probe is at a small angle to the mean flow.

One possible solution to some of the limitations of a conventional fine-wire probe is the use of a small diameter coil of wire for the probe. The springlike properties of the coil allow a higher length-to-diameter ratio for a given flow and minimize strain gage effects. In addition, the coil is more rugged for sudden flow changes. Since a coil can be mounted straight across the support tips there is less support interference in cross flows.

This Note describes such "coil probes" developed for use in a hypersonic helium tunnel. In addition to measuring fluctuating quantities in a boundary layer, these probes were used with a constant temperature anemometer for measuring mean mass flow profiles, and with the constant current anemometer for measuring mean total temperature profiles.

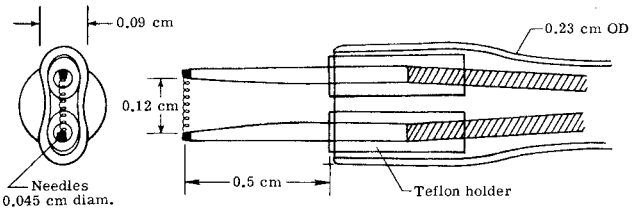

Fig. 1 Hot-wire coil-probe construction.

Probe Construction and Calibration

A small coil of tungsten wire (from a light bulb) was copper plated, stretched across notched needles, and soft soldered to the needle tips. The copper plating between the needles was then removed with nitric acid. The needles were held in a teflon insulator within a small stainless-steel tube. A sketch of a typical probe is shown in Fig. 1. Different size wires and coils were employed with different (l/d)'s, depending on the flow environ-

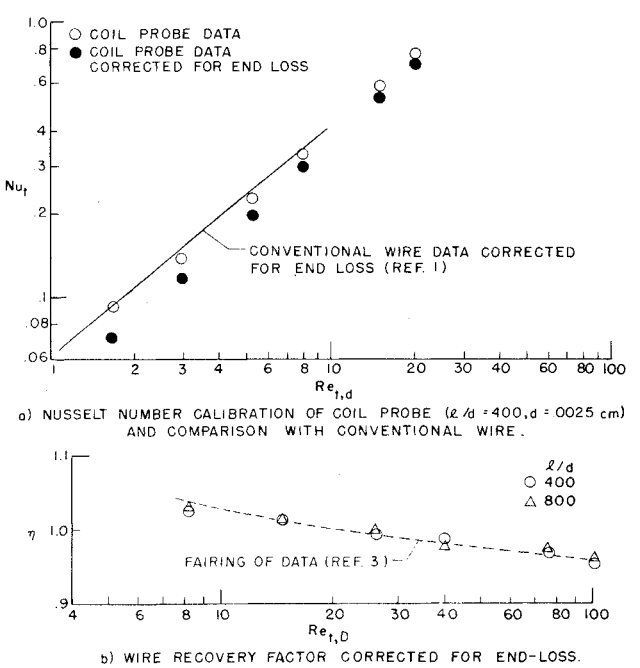

Fig. 2 Typical hot-wire coil-probe calibrations.

Received May 29, 1973, revision received July 11, 1973.

Index categories: Boundary Layers and Convective Heat Transfer—Turbulent; Supersonic and Hypersonic Flow.

* Aerospace Engineer, Applied Fluid Mechanics Section, Hypersonic Vehicles Division.